DOI: 10.1002/ejic.200800235

Synthesis and Spectroscopic Characterization of Organophosphono Derivatives of Lindqvist Niobotungstates – X-ray Crystal Structures of $(n\mathrm{Bu_4N})_3[\mathrm{NbW_{10}O_{38}(RP)_2}]$ (R = *n*Bu, Hep and Ph)

Hafedh Driss,[a,b] Kamal Boubekeur,[b] Mongi Debbabi,*[a] and René Thouvenot*[b]

Keywords: Polyoxometalates / Organic–inorganic hybrid composites / Organophosphono groups / Niobium / Tungsten

A series of organophosphonopolyoxoniobotungstates $[\mathrm{NbW_{10}O_{38}(RP)_2}]^{3-}$ {R = Me (**1**), Et (**2**), Pr (**3**), *n*Bu (**4**), Hex (**5**), Hep (**6**), Cy (**7**), Ph (**8**), All (**9**)} has been prepared by the reaction of $(n\mathrm{Bu_4N})_3[\mathrm{NbW_5O_{19}}]$ with the appropriate organophosphono dichloride, $\mathrm{RP(O)Cl_2}$. All of the products were characterized by infrared and multinuclear (^{31}P and ^{183}W) NMR spectroscopy. Compounds **4**, **6** and **8** were characterized by single-crystal X-ray diffraction. The hybrid anions $[\mathrm{NbW_{10}O_{38}(RP)_2}]^{3-}$ are made up of two $\mathrm{W_5O_{18}}$ subunits, which can be viewed as monovacant derivatives of the niobotungstate precursor linked by a $\{\mathrm{Nb(OPR)_2}\}$ group.

Introduction

Polyoxometalates (POMs) make up a unique class of compounds in terms of compositional and structural diversity. They exhibit remarkable physicochemical properties and are of interest in various fields such as medicine, biology, catalysis, materials science and analytical chemistry.[1] Derivatization with organic groups that can be linked either via noncovalent[2] (e.g., ionic) or covalent[3–5] interactions alters the POM surface, which may be beneficial for various applications, for example, by enhancing the efficiency and selectivity of POM-based catalytic processes.[6] The replacement of hexavalent metal centres, for example $\mathrm{W^{VI}}$, with lower-valent metals (e.g., $\mathrm{Nb^V}$, $\mathrm{V^V}$ or $\mathrm{Ta^V}$) increases the basicity of the neighbouring oxygen atoms as well as the reactivity of the whole polyanion. The enhanced reactivity of these mixed POMs has been largely exploited in the synthesis of hybrid derivatives by grafting organic or organometallic electrophilic moieties.[7] As far as organosilyl and organophosphono derivatives are concerned, Keggin and Dawson POMs have been extensively studied,[8] while for Lindqvist POMs only a few organosilyl derivatives have been reported,[9,10] and to the best of our knowledge nothing has been published on organophosphono derivatives. Our long-standing experience in the synthesis[11] and characterization[12,13] of the series of niobotungstates $[\mathrm{Nb}_x\mathrm{W}_{6-x}\mathrm{O}_{19}]^{(2+x)-}$ ($1 \leq x \leq 4$), led us to investigate their reactivity towards various electrophilic reagents.[10] We report herein the reaction of $(n\mathrm{Bu_4N})_3[\mathrm{NbW_5O_{19}}]$ with a series of organophosphono dichlorides, $\mathrm{RP(O)Cl_2}$. These reactions afford a new family of organic–inorganic hybrids with the general formula $[\mathrm{NbW_{10}O_{38}(RP)_2}]^{3-}$ {R = Me (**1**), Et (**2**), Pr (**3**), *n*Bu (**4**), Hex (**5**), Hep (**6**), Cy (**7**), Ph (**8**), All (**9**)}, which have been characterized by IR and multinuclear NMR spectroscopy and, for some of them, by single-crystal X-ray diffraction.

Results and Discussion

Synthesis and Reactivity

The hexatungstate $[\mathrm{W_6O_{19}}]^{2-}$ is known to be quite stable and inert towards electrophilic attack owing to the weak basicity and nucleophilicity of its oxygen atoms.[14] Substitution of $\mathrm{Nb^V}$ for $\mathrm{W^{VI}}$ results in mixed niobotungstates $[\mathrm{Nb}_x\mathrm{W}_{6-x}\mathrm{O}_{19}]^{(2+x)-}$ with higher reactivity due to the enhanced basicity and nucleophilicity of the oxygen atoms, especially those bound to Nb.[15,16] Indeed, $[\mathrm{NbW_5O_{19}}]^{3-}$ reacts easily with organophosphonic acids $\mathrm{RP(O)(OH)_2}$ or organophosphonic dichlorides $\mathrm{RP(O)Cl_2}$. The reactions were first carried out in polar basic solvents such as dmf, dmso or acetonitrile, which resulted in the formation of $[\mathrm{W_6O_{19}}]^{2-}$ by partial decomposition of $[\mathrm{NbW_5O_{19}}]^{3-}$ and subsequent reaggregation. Hybrid anions of general formula $[\mathrm{NbW_{10}O_{38}(RP)_2}]^{3-}$ were nevertheless obtained in fairly good yield (75 to 90%) by using less polar solvents

[a] Laboratoire de Physico-Chimie des Matériaux. Faculté des Sciences de Monastir,
5019 Monastir, Tunisie
Fax: +216-73-500-514
E-mail: mongi.debbabi@enim.rnu.tn
[b] UPMC Univ Paris 06, Laboratoire de Chimie Inorganique et Matériaux Moléculaires (UMR CNRS 7071), Institut de Chimie Moléculaire (FR 2769), C. 42,
4, place Jussieu, 75005 Paris, France
Fax: +33-1-44273841
E-mail: rene.thouvenot@upmc.fr

Supporting information for this article is available on the WWW under http://www.eurjic.org or from the author.

such as dichloromethane. The formation process of $[NbW_{10}O_{38}(RP)_2]^{3-}$ can be viewed as the (formal) insertion of a RPO group into two Nb–O–W bridges, followed by condensation with elimination of one $\{NbO_2\}$ group.

The reaction of $(nBu_4N)_3[NbW_5O_{19}]$ with $PhP(O)Cl_2$ was monitored in solution by ^{31}P NMR and IR spectroscopy. Addition of solid $(nBu_4N)_3[NbW_5O_{19}]$ to a dilute solution of $PhP(O)Cl_2$ in dichloromethane resulted in the immediate disappearance of the ^{31}P NMR signal for $PhP(O)Cl_2$ (δ = 35 ppm) together with the appearance of numerous signals at lower frequencies (Figure 1). The system evolved progressively towards a final state with essentially two major signals with tungsten satellites (Figure 1e). As the reaction was followed by IR spectroscopy, addition of $PhP(O)Cl_2$ to a suspension of the POM in dichloromethane caused immediate disappearance of the $\nu(Nb–O_t)$ band at 915 cm^{-1} together with a significant splitting of the $\nu_{as}(M–O_b–M')$[17] band at ca. 800 cm^{-1} (Figure 2).[12]

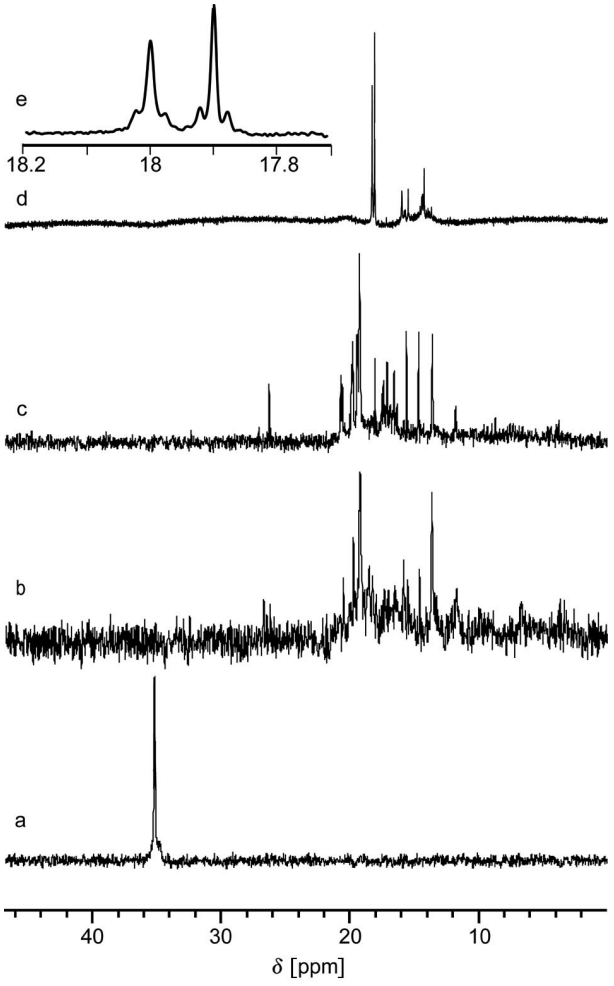

Figure 1. Formation of $[NbW_{10}O_{38}(PhP)_2]^{3-}$ followed by ^{31}P NMR in CD_2Cl_2 solution: (a) $PhP(O)Cl_2$, t = 0, (b) after addition of $(nBu_4N)_3[NbW_5O_{19}]$, t = 2 min, (c) t = 25 min, (d) t = ∞, (e) expansion of the 17.7–18.4 ppm interval of (d).

All these spectroscopic observations indicate that the initial step of grafting $RP(O)Cl_2$ onto $[NbW_5O_{19}]^{3-}$ is very fast, while the formation of the hybrid species requires some hours for completion but no intermediate can be isolated. The hybrid species are moderately soluble in acetonitrile, from which they can be purified by crystallization.

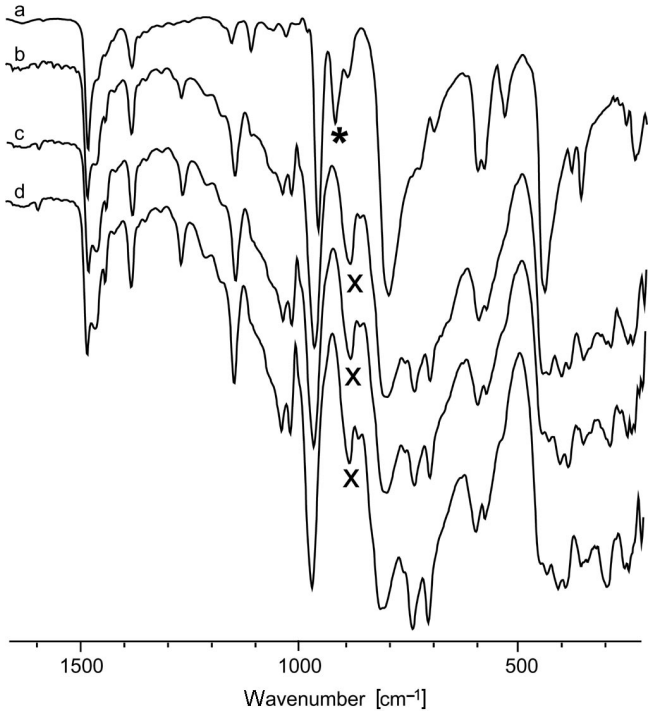

Figure 2. Formation of $[NbW_{10}O_{38}(PhP)_2]^{3-}$ followed by IR spectroscopy in CH_2Cl_2 solution: (a) $(nBu_4N)_3[NbW_5O_{19}]$ (* indicates the $Nb–O_t$ band), (b) after addition of a dilute solution of $PhP(O)Cl_2$ in CH_2Cl_2, t = 2 min, (c) t = 5 min, (d) t = 10 min (× indicates the characteristic vibration of hybrid $(nBu_4N)_3[NbW_{10}O_{38}(RP)_2]$ at 856 cm^{-1}).

IR Spectroscopy

Except for the bands arising from the R group, the IR spectra of all compounds $(nBu_4N)_3[NbW_{10}O_{38}(RP)_2]$ are quite similar in the low-wavenumber region ($\tilde{\nu} < 1100$ cm^{-1}), which is characteristic of the POM framework (Figures 3 and S1, Supporting Information). This strongly suggests that all these compounds have quite similar structures, which is confirmed by multinuclear NMR spectroscopy and X-ray diffraction (vide infra).

The strong features at ca. 970 cm^{-1} [$\nu_{as}(W–O_t)$], 800–860 cm^{-1} [$\nu_{as}(M–O–M)$], 410–440 cm^{-1} and ≈ 350 cm^{-1} [$\nu_{as}(W–O_c)$] are signatures of the Lindqvist structure.[18] Regarding the IR modes of the POM framework, significant changes with respect to $[NbW_5O_{19}]^{3-}$ are the high-frequency shift of the $\nu_{as}(W–O_t)$ band (ca. 10 cm^{-1}), disappearance of the $\nu(Nb–O_t)$ band at 915 cm^{-1} and splitting of the $\nu_{as}(M–O_b–M)$ band by ca. 40 cm^{-1}. This might indicate that the organophosphono groups in the hybrid anion interact, as expected, with O(Nb) atoms only, namely with $O_t(Nb)$ and with some of the adjacent $O_b(NbW)$ atoms. Moreover, stretching and bending modes of the RPO_3 groups appear in the 1000–1200 cm^{-1} and 600–700 cm^{-1} range, respectively.

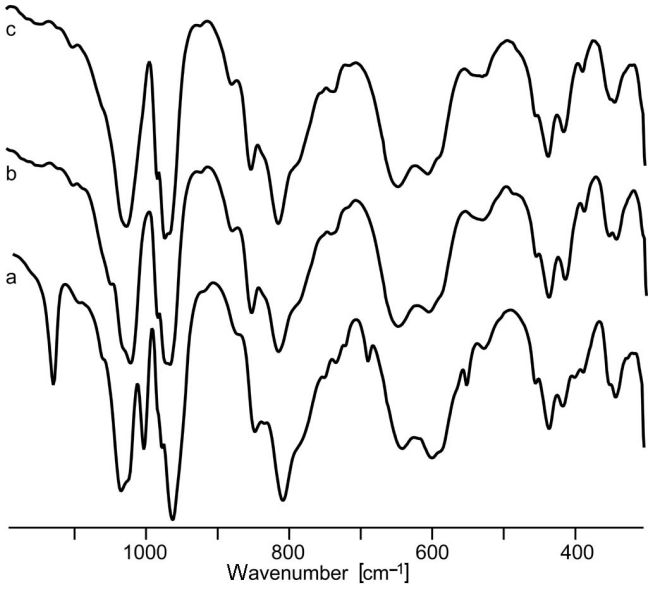

Figure 3. Infrared spectra of $(n\mathrm{Bu_4N})_3[\mathrm{NbW_{10}O_{38}(RP)_2}]$ R = Ph (a), *n*Bu (b) and Hep (c).

X-ray Crystal Structures

Single crystals suitable for X-ray diffraction study were obtained for compounds **4**, **5**, **6** and **8** by slow concentration of their solutions in acetonitrile. Crystal data and details of data collection and refinement are reported in Table 6. Bond lengths and angles are given in Tables 1, 2 and 3. Both alkyl derivatives **4** and **6** crystallize in the chiral $P2_1$ space group, while compound **8** crystallizes in the centrosymmetric $P\bar{1}$ space group. For compound **5**, crystal decomposition during the data collection even at 250 K prevented the determination of the crystal and molecular structure; only cell parameters could be obtained.

The asymmetric unit for **4** and **6** consists of one $[\mathrm{NbW_{10}O_{38}(RP)_2}]^{3-}$ anion and three $(n\mathrm{Bu_4N})^+$ cations in the general position. The hybrid anions of **4** and **6** do not have any crystallographically imposed symmetry. The asymmetric unit of **8** contains three $(n\mathrm{Bu_4N})^+$ cations and two independent halves of the anion, and the central niobium atoms are located on two different inversion centres. Except for the organic moieties, the molecular structures of the anions in compounds **4**, **6** and **8** are quite similar (Figure 4). These anions are built up from two $\{\mathrm{W_5O_{18}}\}$ Lindqvist lacunary moieties connected by a central niobium atom and two {RP} bridging units. Alternatively, the hybrid anions can be described as a niobium(V) coordination complex with two equivalent $\{\mathrm{W_5O_{18}RPO}\}$ entities that act as tridentate ligands in facial configuration with the phosphorus atoms in the *trans* position (Figure 5).

Table 2. P–O bond lengths [Å] and O–P–O and O–P–C angles [°] for $(n\mathrm{Bu_4N})_3[\mathrm{NbW_{10}O_{38}(HepP)_2}]$ (**6**).

P1–O51	1.534(11)	O51–P1–O11	109.47(63)
P1–O11	1.536(11)	O51–P1–O22	112.14(55)
P1–O22	1.544(11)	O51–P1–C1	111.70(69)
P1–C1	1.765(17)	O11–P1–O22	109.90(56)
P2–O21	1.521(11)	O11–P1–C1	106.0(7)
P2–O101	1.546(10)	O22–P1–C1	107.44(65)
P2–O71	1.583(12)	O21–P2–O101	111.10(56)
P2–C8	1.840(16)	O21–P2–O71	110.75(58)
O101–P2–C8	105.73(63)	O21–P2–C8	110.57(61)
O71–P2–C8	107.63(67)	O101–P2–O71	110.88(54)

A more detailed discussion of the structure of the hybrid anions will be restricted to $(n\mathrm{Bu_4N})_3[\mathrm{NbW_{10}O_{38}(HepP)_2}]$ (**6**). The $\mathrm{NbO_6}$ octahedron in **6** is slightly elongated with Nb–O(P) bonds of 2.02 Å, while the four equatorial Nb–O(W) bond lengths range from 1.96 to 1.98 Å. These Nb–O bonds are in the usual range for a single bond with bridging oxygen atoms.[9,10] All O–Nb–O bond angles are close to 90° (Table 1). The $\mathrm{RPO_3}$ tetrahedron represents the classical geometry for organophosphono groups grafted onto polyoxometalate frameworks[5] with P–O(M) and P–C bonds in the range 1.52–1.58 Å and 1.76–1.84 Å, respectively (Table 2).

The lacunary $\{\mathrm{W_5O_{18}}\}$ moieties present *trans* bond-length alternation for the $\mathrm{WO_b}$ bonds (Figure 6a, Table 3), a feature which was already reported in various derivatized Lindqvist anions;[15,19] the difference, Δ, between average long and short bonds within the Nb1–W4–W1–W2–P1 oxo ring is 0.17 Å. No such *trans* bond-length alternation is observed in the equatorial ring, W2–W3–W4–W5 (Figure 6b); on the contrary, the W–O bond lengths along this ring are quite similar with a difference between minimum and maximum values of 0.05 Å. Special mention should be made of the four "surface" oxygen atoms of the lacunary $\{\mathrm{W_5O_{18}}\}$ fragment, i.e., those bound to Nb and P atoms. In the organosilyl derivative $[\mathrm{NbW_5O_{19}SiPh_3}]^{2-}$, the four O–O distances between these oxygen atoms are very similar (2.67 to 2.70 Å, mean value 2.68 Å), which leads to a quasi-square arrangement consistent with the virtual C_{4v} symmetry of the hybrid anion.[10] While in $[\mathrm{NbW_{10}O_{38}(HepP)_2}]^{3-}$ the $\mathrm{O_b}$–$\mathrm{O_b}$ distances within the $\{\mathrm{W_5O_{18}}\}$ framework are also in the same range (2.62 to 2.75 Å, mean value 2.69 Å), coordination of the "surface" oxygen atoms to phosphorus and niobium induces severe deviations from these values. Phosphorus acts as a pincer which forces the O22 and O51 atoms to approach each other, leading to a noticeably short

Table 1. Nb–O bond lengths [Å] and O–Nb–O angles [°] for $(n\mathrm{Bu_4N})_3[\mathrm{NbW_{10}O_{38}(HepP)_2}]$ (**6**).

Nb1–O91	1.962(9)	O91–Nb1–O81	88.35(39)	O81–Nb1–O31	90.86(39)
Nb1–O81	1.962(10)	O91–Nb1–O41	92.44(39)	O81–Nb1–O11	90.06(41)
Nb1–O41	1.978(9)	O91–Nb1–O11	90.15(39)	O81–Nb1–O21	90.17(41)
Nb1–O31	1.983(9)	O91–Nb1–O21	89.24(39)	O41–Nb1–O31	88.34(38)
Nb1–O11	2.022(10)	O31–Nb1–O11	90.61(39)	O41–Nb1–O11	90.21(40)
Nb1–O21	2.025(10)	O31–Nb1–O21	90.00(39)	O41–Nb1–O21	89.57(40)

Table 3. W–O bond lengths [Å] for $(n\text{Bu}_4\text{N})_3[\text{NbW}_{10}\text{O}_{38}(\text{HepP})_2]$ (**6**).

W1–O1	1.724(12)	W3–O3	1.714(12)	W5–O5	1.713(14)
W1–O14	1.840(11)	W3–O31	1.892(12)	W5–O15	1.890(12)
W1–O13	1.877(11)	W3–O23	1.925(10)	W5–O45	1.911(11)
W1–O15	1.989(11)	W3–O34	1.928(11)	W5–O25	1.952(11)
W1–O12	2.021(10)	W3–O13	2.010(12)	W5–O51	2.052(13)
W1–O100	2.273(13)	W3–O100	2.295(11)	W5–O100	2.331(11)
W2–O2	1.700(12)	W4–O4	1.715(13)	W6–O6	1.712(12)
W2–O12	1.864(12)	W4–O41	1.891(12)	W6–O69	1.896(11)
W2–O23	1.915(10)	W4–O34	1.954(11)	W6–O68	1.913(11)
W2–O25	1.920(11)	W4–O45	1.962(11)	W6–O610	2.009(11)
W2–O22	2.048(12)	W4–O14	2.033(12)	W6–O61	2.022(11)
W2–O100	2.305(10)	W4–O100	2.344(11)	W6–O200	2.290(14)
W7–O7	1.674(12)	W8–O8	1.696(11)	W9–O9	1.711(10)
W7–O61	1.874(12)	W8–O78	1.887(11)	W6–O91	1.894(12)
W7–O107	1.922(11)	W8–O81	1.918(12)	W6–O910	1.913(10)
W7–O78	1.934(10)	W8–O89	1.920(11)	W6–O89	1.937(11)
W7–O71	2.018(13)	W8–O68	1.980(11)	W6–O69	1.998(12)
W7–O200	2.292(11)	W8–O200	2.325(11)	W6–O200	2.332(11)
W10–O10	1.698(11)	W10–O910	1.922(10)	W10–O101	2.029(12)
W10–O610	1.883(13)	W10–O107	1.959(12)	W10–O200	2.322(10)

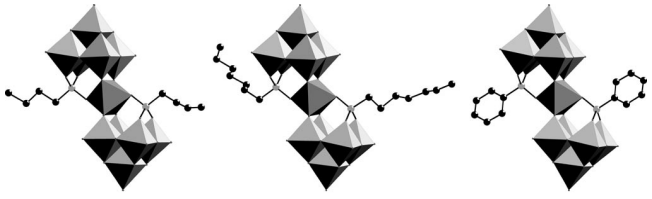

Figure 4. Combined polyhedral and ball-and-stick representation of the molecular structures of $[\text{NbW}_{10}\text{O}_{38}(\text{RP})_2]^{3-}$; from left to right, R = *n*Bu, Hep, Ph.

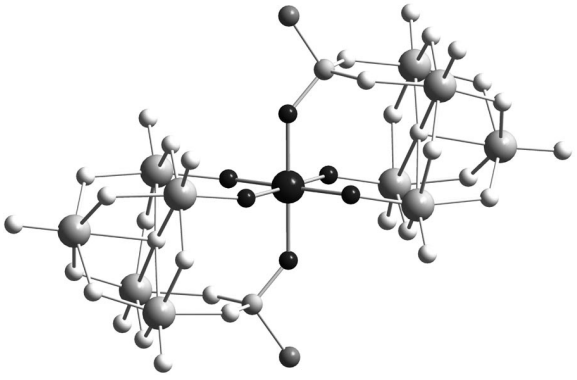

Figure 5. Representation of $[\text{NbW}_{10}\text{O}_{38}(\text{RP})_2]^{3-}$ as a Nb^{V} coordination complex with two tridentate $\{\text{W}_5\text{O}_{18}\text{RPO}\}$ ligands in facial configuration and two RPO groups in *trans* positions.

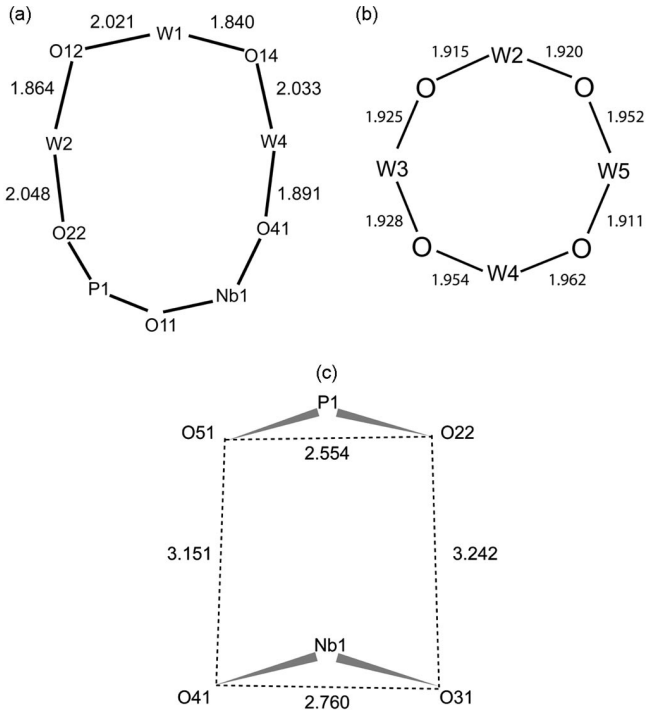

Figure 6. (a) *trans*-Bond alternation along the axial rings Nb1–W4–W1–W2–P1. (b) Regular geometry of the equatorial ring W2–W3–W4–W5. (c) Distortion of the O22–O31–O41–O51 polygon induced by niobium and phosphorus linkage.

O–O distance of 2.55 Å (Figure 6c). Conversely, for the O41 and O31 atoms bound to niobium, there is an increase in *d*(O–O) to 2.76 Å. Moreover, the two other distances, O22–O31 and O41–O51, are especially long (ca. 3.2 Å), because of the steric constraint imposed by the P–O–Nb bridge. All other interatomic distances and bond angles in **6** are usual for polyoxometalate structures. These structural considerations derived from the analysis of metric data of compound **6** are also valid for the two hybrid anions **4** and **8**.

Although there are no crystallographic elements of symmetry for **4** and **6**, and **8** has only inversion centres at the niobium atom positions, all the hybrid anions, excluding the organic part, adopt a geometry consistent with virtual C_{2h} symmetry. The pseudomirror plane is defined by the niobium and the two phosphorus atoms; it also contains the two axial tungsten atoms W1 and W6 and the two central oxygen atoms O100 and O200. This pseudomirror exchanges W2 and W5, W3 and W4, W7 and W10, and W8

and W9. The virtual C_2 axis exchanges the two phosphorus atoms and the two $\{W_5O_{18}\}$ moieties.

This is likely the case for all the obtained compounds, on the basis of the similarity of their IR spectra (vide supra).

^{31}P NMR Spectroscopy

According to the apparent symmetry of the hybrid anion $[NbW_{10}O_{38}(RP)_2]^{3-}$ (C_{2h}), the two phosphorus atoms are equivalent, and a single ^{31}P NMR signal is expected in solution. Actually, this is observed for **1** and **9** only; the $\{^1H\}$-^{31}P NMR spectra of the other hybrid species (**2** to **8**) exhibit two signals with very close chemical shifts ($\Delta\delta$ = 0.1 to 0.2 ppm) (Figure 7, Table 4). The relative integrated intensities of the two resonances depend on R, the high-frequency signal always being less intense than – or at most equal to – the low-frequency one. All these signals display tungsten satellites with ^2J(W–P) coupling constants of 7.4 to 8 Hz; when possible, integration of these satellites with respect to the central line shows that the P atom is connected to two tungsten atoms.

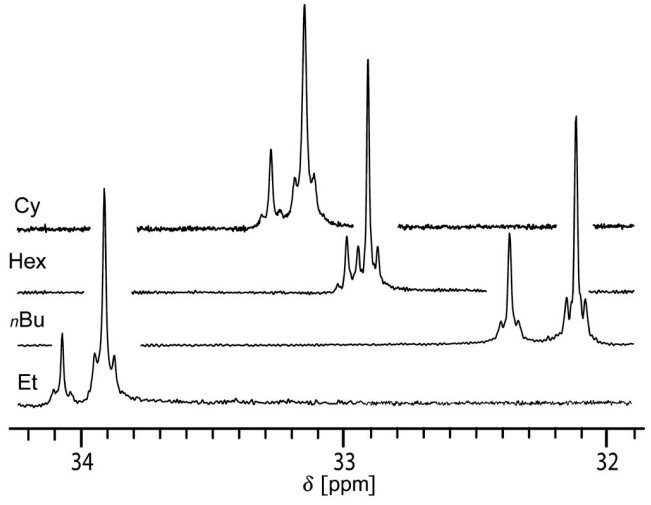

Figure 7. $\{^1H\}$-^{31}P NMR spectra of $[NbW_{10}O_{38}(RP)_2]^{3-}$. Conditions: CD_3CN/CH_3CN, room temperature, 100 g L^{-1}.

Taking into account the ^{31}P chemical shifts, depending on the nature of R, the ^2J(W–P) coupling constants and the relative integrated intensities of the satellites, the structures correspond to RP groups grafted onto the polyoxotungstate surface through two P–O–W bridges.[4,5] The relatively low coupling constants are consistent with the geometry of this bridge with an acute P–O–W angle (ca. 130–135°).[5]

For compounds **2** to **8** the presence of two ^{31}P NMR signals is rather puzzling: (i) the 2-line spectrum is obtained immediately after dissolution of crystallographically pure species, (ii) the spectrum does not evolve at all with time, (iii) crystals obtained from the NMR solution present the same IR spectrum as that of the initial crystals used for the NMR experiment. These observations may be tentatively explained by the presence, in solution, of two species in equilibrium which is established quasi-instantaneously after dissolution of the solid hybrid. Both the rapid equilibrium and very close ^{31}P chemical shifts argue for similar structures for these species. If we consider the NbO_6 octahedron with the two chelating tridentate $\{W_5O_{18}RPO\}$ ligands, the actual X-ray structure of the hybrid anion represents one of the three possible facial configurations, with the two RPO groups in the *trans* position. The two other configurations (Figure 8), with the RPO groups in the *cis* position, may be generated without bond breaking by a Bailar twist-type isomerization process through an intermediate "eclipsed" trigonal prismatic configuration (Scheme 1).[20] Note that these facial configurations are the two enantiomeric forms of the same asymmetric complex, and they must therefore present the same NMR spectrum in an achiral medium. This could explain the experimental ^{31}P NMR spectrum with one signal for the *trans* species and one for the two other enantiomeric *cis* species. For the methyl and allyl derivatives, the *cis–trans* equilibrium might be displaced towards the more stable complex.

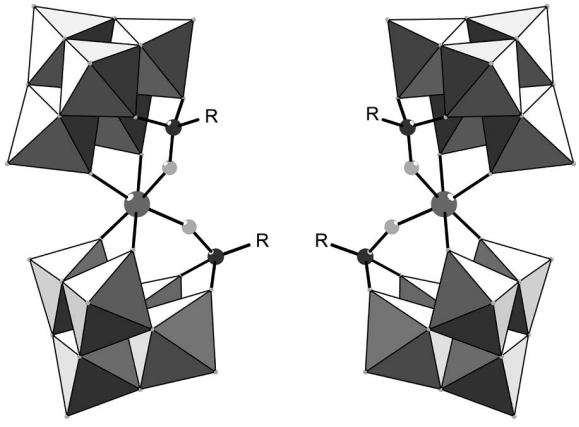

Figure 8. Postulated structures of the two chiral cis isomers of the $[NbW_{10}O_{38}(RP)_2]^{3-}$ hybrid anion.

While the X-ray structural analysis of the well-shaped crystals shows exclusively the *trans* species, the presence of both isomers in the solid material cannot be totally ex-

Table 4. $\{^1H\}$-^{31}P NMR spectroscopic data[a] for $(nBu_4N)_3[NbW_{10}O_{38}(RP)_2]$.

	Me	Et	Pr	Bu	Hex	Hep	Cy	Ph	All	^2J(W–P)[b]
δ(P1)	32.2	33.92	32.76	32.12	32.91	32.04	33.15	17.9	27.09	8
δ(P2)	–	34.07	32.85	32.35	32.98	32.11	33.27	18	–	7.4
δ(P2)–δ(P1)	–	0.15	0.09	0.23	0.07	0.07	0.12	0.1	–	
ρ[c]	–	4	3	2	4	1	5	1	–	

[a] Chemical shifts in ppm relative to 85% H_3PO_4. [b] ^2J(W–P) in Hz. [c] ρ (relative integrated intensity) = I(P1)/I(P2).

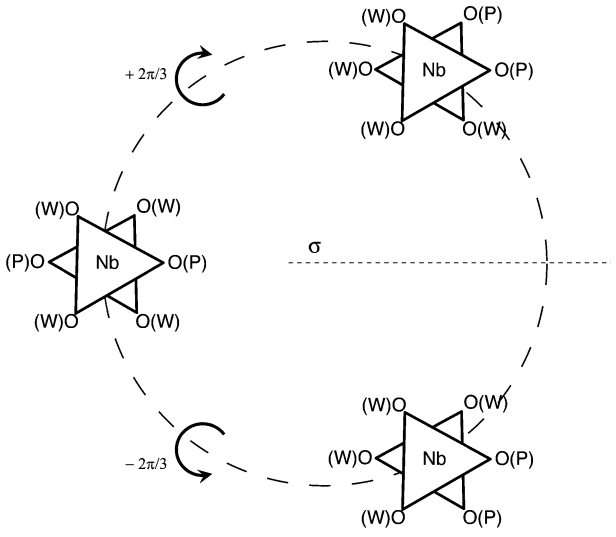

Scheme 1. Scheme of the Bailar twist-type interconversion between the different isomers of $[NbW_{10}O_{38}(RP)_2]^{3-}$.

cluded. A single isotropic signal is observed in the solid-state CP-MAS ^{31}P NMR of the hybrid species; however, regardless of what R is, the linewidth of the signal is more than 300 Hz (ca 2 ppm), which does not allow the identification of the two close resonances, which are at best only 0.2 ppm apart (Figure S2, Supporting Information).

^{183}W NMR Spectroscopy

The low receptivity of the ^{183}W nucleus requires the use of highly concentrated solutions to obtain NMR spectra in a reasonable time interval. The solubility of $(nBu_4N)_3[NbW_{10}O_{38}(RP)_2]$ decreases from dmf and dmso (up to 0.3 mol L^{-1} at room temperature) to CH_3CN (3×10^{-2} mol L^{-1} at room temperature) and CH_2Cl_2. Solutions in dmso or dmf were investigated first and revealed total decomposition of $[NbW_{10}O_{38}(RP)_2]^{3-}$ into yet unidentified products. Attempts were made in acetonitrile at 70 °C, where the solubility is twice that at room temperature. The 20.8 MHz spectrum of $(nBu_4N)_3[NbW_{10}O_{38}(PhP)_2]$ (**8**), obtained after ca. 40 h, shows essentially three broad features ($\Delta\nu_{1/2} \approx 40$ Hz) between 24 and 0 ppm along with two narrow signals at 59.6 ppm ($W_6O_{19}^{2-}$) and –34.2 ppm (unidentified species) (Figure S3, Supporting Information). Using CH_3CN/dmso (ca. 70:30 v/v), in which the solubility at room temperature reaches ca. 8×10^{-2} mol L^{-1}, yields ^{183}W NMR spectra with a satisfactory signal/noise ratio in 5 to 10 h for R = Pr, *n*Bu, Hex and Ph. In these conditions there is nevertheless slow decomposition of the original hybrids, but their ^{183}W resonances could be still identified; for the other compounds, the spectra remained very complex because of advanced decomposition.

The spectrum of $(nBu_4N)_3[NbW_{10}O_{38}(PhP)_2]$ (**8**), obtained in ca. 5 h, is given in Figure S4 (Supporting Information). Two signals at –140.3 and –142.1 ppm, absent in the acetonitrile solution spectrum, correspond to partial decomposition of the hybrid species. The other signals are in the same narrow spectral range as those in the acetonitrile solution spectrum (Figure 9). Surprisingly, the lines of the room-temperature, mixed-solvent spectrum are significantly sharper than those in the high-temperature acetonitrile one; they remain, however, too broad for the observation of tungsten satellites.

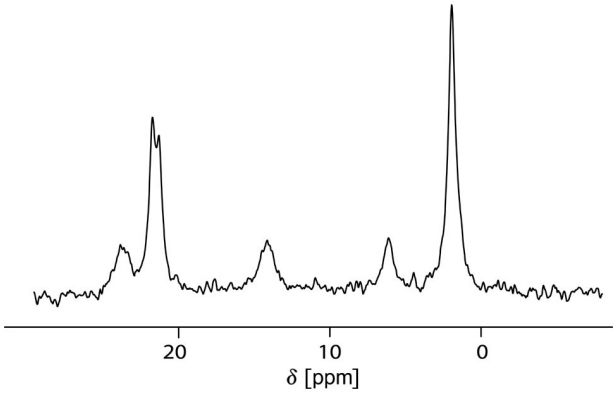

Figure 9. Part of the 20.8 MHz ^{183}W NMR spectrum of $(nBu_4N)_3[NbW_{10}O_{38}(PhP)_2]$. Experimental conditions: T = 300 K, 8×10^{-2} mol L^{-1} in dmso/CD_3CN, 17320 transients, total spectrometer time 5 h. For full spectrum see Figure S3 (Supporting Information).

After analysis of all recorded spectra, a group of three lines in an approximate intensity ratio of 2:1:2 could be assigned to the *trans*-isomer anion in agreement with its apparent C_{2h} symmetry (Table 5). The line at δ = +21.2 ppm appears as a hardly resolved doublet [^2J(W–P) ≈ 10 Hz], which is likely due to coupling with ^{31}P. It could be assigned to the four equivalent W(OP) atoms connected to the phosphono groups. The signal at δ = +1.8 ppm is assigned to the four equivalent W(ONb) atoms connected to niobium and the intermediate signal, with an intensity of ca. 1 (δ = +14.0 ppm), to the apical W(OW) atoms. The two remaining broad lines in the spectrum of **8** could be tentatively ascribed to the chiral *cis*-isomer species; actually, according to the C_2 symmetry of this chiral anion, five ^{183}W signals are expected (two doublets and three singlets with equal intensity), in fact, the local C_s symmetry of each W_5O_{18} moiety would simplify the spectrum to three lines (2:2:1; one doublet, two singlets). In the frame of this hypothesis, the third signal of this species, corresponding to the cap W nuclei, would be missing; however, on the basis of the broadness of the different resonances, the relatively narrow

Table 5. ^{183}W NMR spectroscopic data[a] for $(nBu_4N)_3[NbW_{10}O_{38}(RP)_2]$.

Assignment	R			
	Pr	Bu	Hex	Ph
W(ONb)	+1.5	+1.2	+3.3	+1.8
W(OP)	+19.0	+19.9	+20.2	+21.2
W(OW)	+12.8	+13.1	+14.2	+14.0

[a] Chemical shifts in ppm.

spectral range and the low accuracy of quantification, accidental degeneracy can not be excluded.

Finally, it should be noticed that all tungsten atoms in the hybrid complexes are strongly shielded with respect to the starting $NbW_5O_{19}^{3-}$ species.[10]

Conclusions

A novel series of organophosphonate–polyoxometalate hybrids of general formula $(n\text{Bu}_4\text{N})_3[\text{NbW}_{10}\text{O}_{38}(\text{RP})_2]$ have been obtained by reaction of $(n\text{Bu}_4\text{N})_3[\text{NbW}_5\text{O}_{19}]$ with RP(O)Cl_2 in dichloromethane. These compounds have been characterized in solution (IR and multinuclear NMR) and in the solid state (IR and single-crystal X-ray diffraction). The anions $[\text{NbW}_{10}\text{O}_{38}(\text{RP})_2]^{3-}$ are made up of two W_5O_{18} subunits linked by a $\{\text{Nb(OPR)}_2\}$ group according to C_{2h} symmetry. This new type of hybrid anions can be viewed as resulting from the formal insertion of RPO groups into the Nb–O–W bridges of $NbW_5O_{19}^{3-}$. Further functionalization of the organic groups by coupling reactions would allow preparing extended polymeric networks.

Experimental Section

Analytical grade solvents and organophosphono dichlorides were obtained from commercial sources and used without further purification. $(n\text{Bu}_4\text{N})_3[\text{NbW}_5\text{O}_{19}]$ was prepared according to the literature.[21] All syntheses were performed under an argon atmosphere. Dichloromethane was distilled from $CaCl_2$ and bubbled for 5 min with argon immediately before use.

$(n\text{Bu}_4\text{N})_3[\text{NbW}_{10}\text{O}_{38}(\text{MeP})_2]$ (1): Finely ground $(n\text{Bu}_4\text{N})_3\text{NbW}_5\text{O}_{19}$ (3 g, 1.46 mmol) was suspended in degassed dichloromethane (100 mL). Then, MeP(O)Cl_2 (0.19 mL, 1.46 mmol) was added dropwise, under argon, to the resulting suspension, which was stirred vigorously at room temperature overnight. The mixture becomes homogeneous after ca. 15 min. The clear colourless solution was concentrated by using a rotary evaporator until a viscous oil was obtained. Addition of ethanol (50 mL) to this oil followed by scraping with a glass spatula yielded a white powder. This powder was separated by suction filtration (glass frit porosity 4) and washed successively with ethanol (50 mL) and diethyl ether (50 mL). The crude product was dissolved in a minimum amount of acetonitrile, then ethanol (50 mL) was added, and the precipitated product was collected by suction filtration (glass frit porosity 4), washed successively with ethanol (50 mL) and diethyl ether (50 mL) and dried under vacuum. The white solid was dissolved again in a minimum amount of lukewarm acetonitrile. The clear solution was concentrated to dryness by slow spontaneous evaporation of the solvent. The product was recrystallized twice from acetonitrile. Yield: 1.94 g (78% based on W). $C_{50}H_{114}N_3NbO_{38}P_2W_{10}$ (3358.69): calcd. C 17.9, H 3.4, N 1.2; found C 18.2, H 4.1, N 1.3. IR (KBr pellets, 1200–250 cm^{-1}): $\tilde{\nu}$ = 351 (m), 416 (s), 439 (s), 530 (m), 608 (s), 649 (s), 740 (sh), 816 (vs), 857 (s), 970 (vs, W=O), 1029 (vs, P–O) cm^{-1}.

$(n\text{Bu}_4\text{N})_3[\text{NbW}_{10}\text{O}_{38}(\text{EtP})_2]\cdot 1.5n\text{Bu}_4\text{NCl}$ (2): This compound was prepared by the same procedure as that for **1** by using EtP(O)Cl_2 (0.15 mL, 1.46 mmol) instead of MeP(O)Cl_2. Yield: 2.2 g (88% based on W). $C_{76}H_{172}Cl_{1.5}N_{4.5}NbO_{38}P_2W_{10}$ (3803.61): calcd. C 24.0, H 4.5, N 1.6; found C 23.7, H 4.8, N 1.7. IR (KBr pellets, 1200–250 cm^{-1}): $\tilde{\nu}$ = 274 (s), 419 (s), 441 (s), 606 (s), 658 (s), 740 (sh), 817 (vs), 856 (s), 969 (vs, W=O), 1025 (s, P–O), 1060 (s), 1093 (sh) cm^{-1}.

$(n\text{Bu}_4\text{N})_3[\text{NbW}_{10}\text{O}_{38}(n\text{PrP})_2]\cdot n\text{Bu}_4\text{NCl}$ (3): This compound was prepared by the same procedure as that for **1** by using $n\text{PrP(O)Cl}_2$ (0.18 mL, 1.46 mmol) instead of MeP(O)Cl_2. Yield: 2.1 g (83% based on W). $C_{70}H_{158}ClN_4NbO_{38}P_2W_{10}$ (3692.71): calcd. C 22.8, H 4.3, N 1.5; found C 22.6, H 4.3, N 1.5. IR (KBr pellets, 1200–250 cm^{-1}): $\tilde{\nu}$ = 276 (s), 416 (s), 437 (s), 526 (m), 607 (s), 661 (s), 753 (sh), 815 (vs), 855 (s), 971 (vs, W=O), 1023 (vs, P–O), 1044 (sh), 1109 (s) cm^{-1}.

$(n\text{Bu}_4\text{N})_3[\text{NbW}_{10}\text{O}_{38}(n\text{BuP})_2]$ (4): This compound was prepared by the same procedure as that for **1** by using $n\text{BuP(O)Cl}_2$ (0.2 mL, 1.46 mmol) instead of MeP(O)Cl_2. Yield: 2.1 g (83% based on W). $C_{56}H_{126}N_3NbO_{38}P_2W_{10}$ (3442.85): calcd. C 19.5, H 3.7, N 1.2; found C 20.4, H 3.8, N 1.2. IR (KBr pellets, 1200–250 cm^{-1}): $\tilde{\nu}$ = 276 (s), 412 (s), 435 (s), 529 (w), 593 (s), 617 (s), 691 (s), 740 (sh), 831 (s), 858 (s), 971 (vs, W=O), 1030 (vs, P–O), 1124 (w), 1147 (m) cm^{-1}.

$(n\text{Bu}_4\text{N})_3[\text{NbW}_{10}\text{O}_{38}(n\text{HexP})_2]$ (5): This compound was prepared by the same procedure as that for **1** by using $n\text{HexP(O)Cl}_2$ (0.25 mL, 1.46 mmol) instead of MeP(O)Cl_2. Yield: 2.3 g (89% based on W). $C_{60}H_{134}N_3NbO_{38}P_2W_{10}$ (3498.95): calcd. C 20.6, H 3.9, N 1.2; found C 20.7, H 3.2, N 1.4. IR (KBr pellets, 1200–250 cm^{-1}): $\tilde{\nu}$ = 275 (s), 414 (s), 436 (s), 528 (m), 607 (s), 649 (s), 744 (sh), 817 (vs), 855 (s), 969 (vs, W=O), 1031 (vs, P–O), 1160 (w) cm^{-1}.

$(n\text{Bu}_4\text{N})_3[\text{NbW}_{10}\text{O}_{38}(n\text{HepP})_2]$ (6): This compound was prepared by the same procedure as that for **1** by using $n\text{HepP(O)Cl}_2$ (0.32 g, 1.46 mmol) instead of MeP(O)Cl_2. Yield: 2.2 g (85% based on W). $C_{62}H_{138}N_3NbO_{38}P_2W_{10}$ (3527.01): calcd. C 21.1, H 3.9, N 1.2; found C 20.9, H 3.8, N 1.5. IR (KBr pellets, 1200–250 cm^{-1}): $\tilde{\nu}$ = 352 (m), 414 (s), 438 (s), 529 (w), 609 (s), 624 (s), 736 (sh), 826 (s), 856 (s), 969 (vs, W=O), 1022 (s, P–O), 1064 (s), 1160 (w) cm^{-1}.

$(n\text{Bu}_4\text{N})_3[\text{NbW}_{10}\text{O}_{38}(\text{CyP})_2]$ (7): This compound was prepared by the same procedure as that for **1** by using CyP(O)Cl_2 (0.29 g, 1.46 mmol) instead of MeP(O)Cl_2. Yield: 2 g (78% based on W). $C_{60}H_{130}N_3NbO_{38}P_2W_{10}$ (3494.92): calcd. C 20.6, H 3.7, N 1.2; found C 20.0, H 3.7, N 1.2. IR (KBr pellets, 1200–250 cm^{-1}): $\tilde{\nu}$ = 275 (m), 414 (s), 437 (s), 530 (mw), 605 (s), 650 (s), 744 (sh), 818 (vs), 856 (s), 970 (vs, W=O), 1026 (vs, P–O), 1107 (w), 1152 (w) cm^{-1}.

$(n\text{Bu}_4\text{N})_3[\text{NbW}_{10}\text{O}_{38}(\text{PhP})_2]\cdot n\text{Bu}_4\text{NCl}$ (8): This compound was prepared by the same procedure as that for **1** by using PhP(O)Cl_2 (0.2 mL, 1.46 mmol) instead of MeP(O)Cl_2. Yield: 2.3 g (90% based on W). $C_{76}H_{154}ClN_4NbO_{38}P_2W_{10}$ (3760.74): calcd. C 24.3, H 4.1, N 1.5; found C 24.0, H 3.8, N 1.4. IR (KBr pellets, 1200–250 cm^{-1}): $\tilde{\nu}$ = 275 (s), 414 (s), 436 (s), 530 (m), 605 (s), 648 (s), 740 (sh), 818 (s), 858 (s), 970 (vs, W=O), 1026 (vs, P–O), 1107 (w), 1159 (w) cm^{-1}.

$(n\text{Bu}_4\text{N})_3[\text{NbW}_{10}\text{O}_{38}(\text{AllP})_2]$ (9): This compound was prepared by the same procedure as that for **1** by using AllP(O)Cl_2 (0.17 mL, 1.46 mmol) instead of MeP(O)Cl_2. Yield: 1.9 g (75% based on W). $C_{54}H_{118}N_3NbO_{38}P_2W_{10}$ (3410.76): calcd. C 19.0, H 3.5, N 1.2; found C 20.2, H 3.3, N 1.2. IR (KBr pellets, 1200–250 cm^{-1}): $\tilde{\nu}$ = 276 (s), 411 (s), 432 (s), 524 (w), 585 (s), 602 (s), 736 (sh), 816 (s), 855 (s), 968 (vs, W=O), 1020 (vs, P–O), 1149 (w), 1640 (m) cm^{-1}.

X-ray Crystal Structure Analysis: Suitable single crystals of **4**, **5**, **6** and **8** for X-ray structure determination were obtained by slow concentration of corresponding solution in acetonitrile. In each

Table 6. Crystal data and structure refinement for **4**, **5**, **6** and **8**.

	4	**5**[a]	**6**	**8**
CCDC deposit no	669713		669714	669715
Formula	$C_{56}H_{126}N_3NbO_{38}P_2W_{10}$	$C_{60}H_{134}N_3NbO_{38}P_2W_{10}$	$C_{62}H_{138}N_3NbO_{38}P_2W_{10}$	$C_{60}H_{118}N_3NbO_{38}P_2W_{10}$
M [g mol^{-1}]	3442.96	3498.95	3527.01	3482.83
Crystal system	monoclinic	monoclinic	monoclinic	triclinic
Space group	$P2_1$ (No. 4)	–	$P2_1$ (No. 4)	$\bar{P}1$ (No. 2)
a [Å]	11.8460(15)	11.8220(3)	11.9080(13)	12.039(2)
b [Å]	32.544(3)	33.3132(6)	34.423(4)	19.4500(10)
c [Å]	12.5570(8)	12.4557(4)	12.6680(15)	24.125(3)
α [°]	90	90	90	70.616(9)
β [°]	103.421(9)	102.745(3)	102.969(8)	82.145(9)
γ [°]	90	90	90	80.294(7)
V [Å^3]	4708.7(8)	4784.5(5)	5060.3(10)	5232.8(11)
Z	2	–	2	2
μ [cm^{-1}]	12.380	–	11.527	11.141
$\rho_{calcd.}$ [g cm^{-1}]	2.428	–	2.315	2.10
θ range [°]	1.767–27.503	–	3.20–30.0	2.13–30.0
Index range	$-14 < h < 15$, $-42 < k < 42$, $-16 < l < 13$	–	$-14 < h < 16$, $-48 < k < 46$, $-17 < l < 17$	$-16 < h < 16$, $-27 < k < 27$, $-33 < l < 33$
Refl. collected	41870	–	43898	111761
Used reflections	19960	–	26929	30313
Reflections with $I > 2\sigma(I)$	14123	–	16602	14780
Parameters refined	706	–	734	799
Goodness of fit S	0.961	–	0.972	0.991
$R[F^2 > 2\sigma(F^2)]$	0.0587	–	0.0502	0.0635
$wR(F^2)$[b]	0.1421	–	0.0998	0.1741

[a] Crystal decomposition during data collection. [b] The weighted R-factor wR and goodness of fit S are based on F^2. Weighting details: $w = 1/[\sigma^2(F_o^2) + (aP)^2 + bP]$ where $P = (F_o^2 + 2F_c^2)/3$. a = 0.0868, 0.0457, 0.1099 Å; b = 35.7431, 0.00, 40.1271 Å for **4**, **6** and **8**, respectively.

case, a colourless prismatic crystal was selected and mounted on an Enraf–Nonius Kappa-CCD diffractometer using graphite-monochromated Mo-K_α radiation (λ = 0.71073 Å). Data were collected at 250 K. Refinement of cell parameters has been performed by Dirax/lsq (Duisenberg & Schreurs, 1989–2000) and data reduction by EvalCCD (Duisenberg & Schreurs 1990–2000). The crystal data and details of data collection and structure refinement are summarized in Table 6. The structures were solved by direct methods (metal atoms and most of the oxygen atoms of the anions) by using SHELXS86.[22] The structures were refined by full-matrix least-squares techniques (on F^2) and difference-Fourier maps (the remaining non-hydrogen atoms) by using SHELXL97[23] and CRYSTALS.[24] The H atoms were simply introduced at idealized positions (riding model) in the structure factor calculations. Molecular structures were drawn with Diamond.[25]

CCDC-669713, -669714 and -669715 contain the supplementary crystallographic data for this paper for compounds **4**, **6** and **8**, respectively. These data can be obtained free of charge from The Cambridge Crystallographic Data Centre via www.ccdc.cam.ac.uk/data_request/cif.

^{183}W NMR Spectroscopy: ^{183}W NMR spectra were recorded in 10-mm o.d. tubes at 20.8 MHz with a Bruker DRX500 spectrometer. Chemical shifts are given with respect to an external Na_2WO_4 solution (2 M) in alkaline D_2O, by using a saturated solution of dodecatungstosilicic acid ($SiW_{12}O_{40}H_4$) as a secondary standard (δ = –103.8 ppm).

^{31}P NMR Spectroscopy: ^{31}P NMR spectra were recorded in 5-mm o.d. tubes at 121.49 MHz with a Bruker AC300 spectrometer equipped with a QNP probe head. The chemical shifts are given according to the IUPAC convention, with respect to 85% H_3PO_4.

IR Spectroscopy: IR spectra of the solid samples were recorded from KBr pellets with a Bio-Rad FTS 165 FT-IR spectrometer with a resolution of 4 cm^{-1}. The formation of the hybrids was monitored with a Bruker Tensor 27 FT-IR spectrometer equipped with a diamond ATR accessory.

Supporting Information (see footnote on the first page of this article): IR spectra of **1** to **9** (Figure S1), solid-state CP-MAS ^{31}P NMR spectrum of **8** (Figure S2), ^{183}W NMR spectra of **8** in acetonitrile (Figure S3) and in mixed acetonitrile/dmso solution (Figure S4).

Acknowledgments

This work was supported by the Centre National de Recherche Scientifique CNRS (France) and the Direction Générale de la Recherche Scientifique DGRST (Tunisia) in the frame of a bilateral joint project. We greatly acknowledge the Comité Mixte pour la Coopération Universitaire (CMCU program 05G1211). We are also grateful to Patrick Herson (UPMC) for crystal data collection and for his assistance in structure resolution.

[1] P. Souchay, *Ions Minéraux Condensés*, Masson, Paris, **1969**; M. T. Pope, *Heteropoly and Isopoly Oxometalates*, Springer-Verlag, Berlin, **1983**; P. Gouzerh, M. Che, *L'actualité chimique* **2006**, *298*, 9–22; J. T. Rhule, C. L. Hill, D. A. Judd, R. F. Schinazi, *Chem. Rev.* **1998**, *98*, 327–358; C. L. Hill, *J. Mol. Catal. A* **2007**, *262*, 2–6.

[2] S. Triki, L. Ouahab, J. Padiou, D. Grandjean, *J. Chem. Soc., Chem. Commun.* **1989**, 1068–1070.

[3] a) V. W. Day, W. G. Klemperer, D. J. Maltbie, *Organometallics* **1985**, *4*, 104–111; b) A. Mazeaud, N. Ammari, F. Robert, R.

Thouvenot, *Angew. Chem. Int. Ed. Engl.* **1996**, *35*, 1961–1964.
[4] a) C. R. Mayer, R. Thouvenot, *J. Chem. Soc., Dalton Trans.* **1998**, 7–13; b) G. S. Kim, K. S. Hagen, C. L. Hill, *Inorg. Chem.* **1992**, *31*, 5316–5324.
[5] C. R. Mayer, P. Herson, R. Thouvenot, *Inorg. Chem.* **1999**, *38*, 6152–6158.
[6] a) D. E. Katsoulis, *Chem. Rev.* **1998**, *98*, 359–388; b) A. Proust, R. Thouvenot, P. Gouzerh, *Chem. Commun.* **2008**, 1837–1852.
[7] R. G. Finke, S. Ozkar, *Coord. Chem. Rev.* **2004**, *248*, 135–146; B. M. Rapko, M. Pohl, R. G. Finke, *Inorg. Chem.* **1994**, *33*, 3625–3634; E. V. Radkov, R. H. Beer, *Inorg. Chim. Acta* **2000**, *297*, 191–198; C. J. Besecker, V. W. Day, W. G. Klemperer, M. R. Thompson, *J. Am. Chem. Soc.* **1984**, *106*, 4125–4136; A. V. Besserguenev, M. H. Dickman, M. T. Pope, *Inorg. Chem.* **2001**, *40*, 2582–2586.
[8] For a recent review on – inter alia – organosilyl and organophosphono derivatives see ref.[6b] Among the abundant literature for Keggin and Dawson POMs, see ref.[3b,4,5] and: W. H. Knoth, *J. Am. Chem. Soc.* **1979**, *101*, 759–760; P. Judeinstein, C. Deprun, L. Nadjo, *J. Chem. Soc., Dalton Trans.* **1991**, 1991–1997; M. S. Weeks, C. L. Hill, R. F. Schinazi, *J. Med. Chem.* **1992**, *35*, 1216; D. A. Judd, R. F. Schinazi, C. L. Hill, *Antiviral Chem. Chemother.* **1994**, *5*, 410–414; S. Shigeta, S. Mori, J. Watanabe, M. Baba, A. M. Khenkin, C. L. Hill, R. F. Schinazi, *Antiviral Chem. Chemother.* **1995**, *6*, 114–122; Z.-G. Sun, Q. Liu, J.-F. Liu, *Polyhedron* **2000**, *19*, 125–128; Z.-G. Sun, Q. Liu, J.-F. Liu, *Inorg. Chem. Commun.* **2000**, *3*, 328–330; C. R. Mayer, I. Fournier, R. Thouvenot, *Chem. Eur. J.* **2000**, *6*, 105–110; Z. Sun, Q. Liu, J. Liu, *Transition Met. Chem.* **2000**, *25*, 374–376; Z.-G. Sun, W.-S. You, J. Li, J.-F. Liu, *Inorg. Chem. Commun.* **2003**, *6*, 238–240; Z.-G. Sun, Z.-M. Zhu, W.-S. You, J.-F. Liu, *Transition Met. Chem.* **2003**, *28*, 849–851;z) C. R. Mayer, C. Roch-Marchal, H. Lavanant, R. Thouvenot, N. Sellier, J. C. Blais, F. Sécheresse, *Chem. Eur. J.* **2004**, *10*, 5517–5523; T. Hasegawa, K. Shimizu, H. Seki, H. Murakami, S. Yoshida, K. Yoza, K. Nomiya, *Inorg. Chem. Commun.* **2007**, *10*, 1140–1144; D. Agustin, J. Dallery, C. Coelho, A. Proust, R. Thouvenot, *J. Organomet. Chem.* **2007**, *692*, 746–754.
[9] V. W. Day, W. G. Klemperer, C. Schwartz, *J. Am. Chem. Soc.* **1987**, *109*, 6030–6044.
[10] F. Bannani, R. Thouvenot, M. Debbabi, *Eur. J. Inorg. Chem.* **2007**, 4357–4363.
[11] M. Dabbabi, M. Boyer, *J. Inorg. Nucl. Chem.* **1976**, *38*, 1011–1014.
[12] C. Rocchiccioli-Deltcheff, R. Thouvenot, M. Dabbabi, *Spectrochim. Acta Part A* **1977**, *33*, 143–153.
[13] M. Dabbabi, M. Boyer, J.-P. Launay, Y. Jeannin, *J. Electroanal. Chem.* **1977**, *76*, 153–164.
[14] L. Barcza, M. T. Pope, *J. Phys. Chem.* **1975**, *79*, 92–93.
[15] T. M. Che, V. W. Day, L. C. Francesconi, M. F. Fredrich, W. G. Klemperer, W. Shum, *Inorg. Chem.* **1985**, *24*, 4055–4062.
[16] C. J. Besecker, V. W. Day, W. G. Klemperer, M. R. Thompson, *Inorg. Chem.* **1985**, *24*, 44–50.
[17] O_t, O_b and O_c correspond to terminal, bridging and central oxygen atoms, respectively.
[18] R. Mattes, H. Bierbüsse, J. Fuchs, *Z. Anorg. Allg. Chem.* **1971**, *385*, 230–242; C. Rocchiccioli-Deltcheff, R. Thouvenot, M. Fouassier, *Inorg. Chem.* **1982**, *21*, 30–35.
[19] C. Bustos, B. Hasenknopf, R. Thouvenot, J. Vaissermann, A. Proust, P. Gouzerh, *Eur. J. Inorg. Chem.* **2003**, 2757–2766.
[20] J. C. Bailar, *J. Inorg. Nucl. Chem.* **1958**, *8*, 165–175; R. W. Saalfrank, B. Demleitner, H. Glaser, H. Maid, D. Bathelt, F. Hampel, W. Bauer, M. Teichert, *Chem. Eur. J.* **2002**, *8*, 2679–2683.
[21] F. Bannani, H. Driss, R. Thouvenot, M. Debbabi, *J. Chem. Crystallogr.* **2007**, *37*, 37–48.
[22] G. M. Sheldrick, *SHELXS86: Program for the Solution of Crystal Structure*, University of Göttingen, Germany, **1986**.
[23] G. M. Sheldrick, *SHELXL97: Program for the Refinement of Crystal Structure*, University of Göttingen, Germany, **1997**.
[24] a) D. J. Watkin, C. K. Prout, J. R. Carruthers, P. W. Betteridge, R. I. Cooper, *CRYSTALS: Single Crystal X-ray Structure Refinement and Analysis*, Chemical Cristallography Laboratory, University of Oxford, **2003**; b) P. W. Betteridge, J. R. Carruthers, R. I. Cooper, K. Prout, D. J. Watkin, *J. Appl. Crystallogr.* **2003**, *36*, 1487.
[25] K. Brandenburg, *DIAMOND*, Gerhard-Domagk-Strasse 1, 53121 Bonn, Germany, **1998**.

Received: March 5, 2008
Published Online: July 7, 2008

